

See discussions, stats, and author profiles for this publication at: <https://www.researchgate.net/publication/26725454>

Biodegradable Thermogelling Poly[(R)-3-hydroxybutyrate]-Based Block Copolymers: Micellization, Gelation, and Cytotoxicity and Cell Culture Studies

ARTICLE in THE JOURNAL OF PHYSICAL CHEMISTRY B · SEPTEMBER 2009

Impact Factor: 3.3 · DOI: 10.1021/jp903984r · Source: PubMed

CITATIONS

34

READS

21

3 AUTHORS, INCLUDING:



Xian Jun Loh

Agency for Science, Technology and Resea...

102 PUBLICATIONS 2,470 CITATIONS

SEE PROFILE



Jing Li

Jilin University

800 PUBLICATIONS 20,585 CITATIONS

SEE PROFILE

Biodegradable Thermogelling Poly[(R)-3-hydroxybutyrate]-Based Block Copolymers: Micellization, Gelation, and Cytotoxicity and Cell Culture Studies

Xian Jun Loh,^{†,‡,§} Suat Hong Goh,^{||} and Jun Li^{*,†,‡,§}

Division of Bioengineering, Faculty of Engineering, National University of Singapore (NUS), 7 Engineering Drive 1, Singapore 117574, Singapore, NUS Graduate School for Integrative Sciences and Engineering (NGS), 28 Medical Drive, Singapore 117456, Singapore, Institute of Materials Research and Engineering, A*STAR (Agency for Science, Technology and Research), 3 Research Link, Singapore 117602, Singapore, and Department of Chemistry, Faculty of Science, National University of Singapore, 3 Science Drive 3, Singapore 117543, Singapore

Received: April 30, 2009; Revised Manuscript Received: July 17, 2009

A series of biodegradable multiblock poly(ester urethane)s having poly[(R)-3-hydroxybutyrate] (PHB), poly(ethylene glycol) (PEG), and poly(propylene glycol) (PPG) segments was prepared. The critical micellization concentration (CMCs) of these water-soluble poly(ester urethane)s were determined at different temperatures in order to calculate the thermodynamic parameters for the process of micelle formation. The process for micelle formation was found to be entropy-driven. The thermogelling behavior of the aqueous polymer solution was studied by ¹H and ¹³C NMR spectroscopy at different temperatures. We obtained valuable molecular level information regarding the state of the copolymer in solution based on the variation of the peak widths. Cytotoxicity studies performed on the extracts of the copolymer gel indicate good cell compatibility. Cells attach on the surface of the gel much better than on the commercially available PEG–PPG–PEG triblock copolymer. These studies indicate a potential for the copolymer gel to be used for tissue engineering applications.

Introduction

Thermogelling copolymers can be applied in areas such as sustained drug delivery, gene delivery, and tissue engineering.^{1–7} Currently, poly(ethylene glycol)-*block*-poly(propylene glycol)-*block*-poly(ethylene glycol) (PEG–PPG–PEG) triblock copolymers (commonly known as Pluronics) are the most widely used commercial thermogelling copolymers. They have been used for controlled drug delivery, wound covering, and chemosensitizing for cancer therapy.^{8–10} However, they are not biodegradable. Other disadvantages of Pluronics include burst release of bioactive agents encapsulated within the gel as well as poor gel stability *in vivo*.^{11,12} Generally, biodegradability is an issue that practitioners consider when using these thermogelling copolymers in biomedical systems. In an ideal scenario, the gel should be completely removed from the body after its period of application. The size of a biodegradable polymer can be reduced by hydrolysis, and the polymer fragments can then be excreted from the body. Biodegradability can be introduced into copolymers by incorporating hydrolyzable segments, such as poly(ϵ -caprolactone) or poly(lactic acid) in the copolymer. There have been many reports of biodegradable thermogelling copolymers in recent literature.^{13–22} Extensive reviews on thermogelling copolymers have recently been published.^{7,23}

Recently, our laboratory has synthesized thermogelling poly(ester urethane)s comprising PEG, PPG, and PHB.²⁰ The

hydrolytic degradation as well as the drug release properties of this new thermogelling copolymer were reported.²¹ However, the process of micellization as well as gelation of the copolymer solution is still poorly understood. Moreover, while this copolymer has potential biomedical applications, we have yet to report cell culture studies on this material. A recent study has reported poor cell adhesion on Pluronic gel.²⁴ In this paper, we have studied the thermodynamics of the micellization process based on the change in the critical micelle concentration (CMC) of the copolymer solution at different temperatures. We report, as well, a deeper understanding of the gelation process based on ¹H and ¹³C NMR spectroscopic studies carried out at various temperatures. Finally, we show that the incorporation of small amounts of PHB segments into the copolymer significantly enhances the cell adhering ability of the copolymer, when compared to the Pluronic gel. The findings have significant implications in the development of thermogelling copolymers for tissue engineering applications.

Experimental Section

Materials. Natural source poly[(R)-3-hydroxybutyrate] (PHB) was supplied by Aldrich, and purified by dissolving in chloroform followed by filtration and subsequent precipitation in hexane before use. The M_n and M_w of the purified PHB were 8.7×10^4 and 2.3×10^5 , respectively. Poly(ethylene glycol) (PEG) and poly(propylene glycol) (PPG) with an M_n value of ca. 2000 was purchased from Aldrich. Purification of the PEG was performed by dissolving in dichloromethane followed by precipitation in diethyl ether and vacuum-dried before use. Purification of PPG was performed by washing in hexane three times and vacuum-dried before use. The M_n and M_w values of PEG were found to be 1890 and 2060, respectively. The M_n and M_w values of PPG were found to be 2180 and 2290,

* Corresponding author. E-mail: bielj@nus.edu.sg. Phone: +65-6516-7273. Fax: +65-6872-3069.

[†] Division of Bioengineering, Faculty of Engineering, National University of Singapore (NUS).

[‡] NUS Graduate School for Integrative Sciences and Engineering (NGS).

[§] A*STAR (Agency for Science, Technology and Research).

^{||} Department of Chemistry, Faculty of Science, National University of Singapore.

TABLE 1: Molecular Characteristics of Poly(PEG/PPG/PHB urethane)s

copolymer ^b	M_n^c ($\times 10^3$)	M_w/M_n^c	copolymer composition ^a (wt %)		
			PEG	PPG	PHB
EPH1	50.6	1.56	64.0	33.9	2.1
EPH2	45.5	1.38	57.0	37.9	5.1
EPH3	42.5	1.37	56.3	35.6	8.1

^a Calculated from ¹H NMR results. ^b Poly(PEG/PPG/PHB urethane)s are denoted EPH, E for PEG, P for PPG, and H for PHB. The M_n of PEG, PPG, and PHB used for the copolymer synthesis was 1890, 2180, and 1070 g mol⁻¹, respectively. ^c Determined by GPC.

respectively. Bis(2-methoxyethyl) ether (diglyme, 99%), ethylene glycol (99%), dibutyltin dilaurate (95%), 1,6-hexamethylene diisocyanate (HDI) (98%), methanol, diethyl ether, 1,2-dichloroethane (99.8%), and 1,6-diphenyl-1,3,5-hexatriene (DPH) were purchased from Aldrich. Diglyme was dried with molecular sieves, and 1,2-dichloroethane was distilled over CaH₂ before use. PEG-PPG-PEG triblock copolymer with a chain composition of EG₁₀₀PG₆₅EG₁₀₀ (also known as Pluronic F127) was purchased from Aldrich and used as received.

Synthesis of Poly(PEG/PPG/PHB urethane)s. Telechelic hydroxylated PHB (PHB-diol) prepolymers with a molecular weight of 1070 g mol⁻¹ was prepared by transesterification using the natural source PHB and ethylene glycol using dibutyltin dilaurate in diglyme as reported previously.^{20,21,25–27} The yield was about 80%. Poly(PEG/PPG/PHB urethane)s were synthesized from PHB-diol, PEG, and PPG with molar ratios of PEG/PPG fixed at 2:1 and PHB content ranging from about 3 to 9 mol % (calculated from the M_n value of PHB-diol) using HDI as a coupling reagent. The amount of HDI added was equivalent to the reactive hydroxyl groups in the solution. Typically, 0.064 g of PHB-diol (M_n = 1070, 6.0×10^{-5} mol), 1.44 g of PEG (M_n = 1890, 7.6×10^{-4} mol), and 0.82 g of PPG (M_n = 2180, 3.8×10^{-4} mol) were dried in a 250 mL two-neck flask at 50 °C under high vacuum overnight. Then, 20 mL of anhydrous 1,2-dichloroethane was added to the flask and any trace of water in the system was removed through azeotropic distillation with only 1 mL of 1,2-dichloroethane being left in the flask. When the flask was cooled down to 75 °C, 0.20 g of HDI (1.2×10^{-3} mol) and two drops of dibutyltin dilaurate ($\sim 8 \times 10^{-3}$ g) were added sequentially. The reaction mixture was stirred at 75 °C under a nitrogen atmosphere for 48 h. The resultant copolymer was precipitated from diethyl ether, and further purified by redissolving into 1,2-dichloroethane followed by precipitation in a mixture of methanol and diethyl ether to remove the remaining dibutyltin dilaurate. A series of poly(PEG/PPG/PHB urethane)s with different compositions of PHB were prepared, and their number-average molecular weight and polydispersity values are given in Table 1. The yield was 80% and above after isolation and purification. ¹H NMR (CDCl₃) of poly(PEG/PPG/PHB urethane)s EPH2: δ (ppm) 1.14 (–O(CH₂)CHCH₂O–), 1.26 (–O(CH₂)CHCH₂CO–), 1.32 (–OOCNHCH₂CH₂CH₂CH₂NHCOO–), 1.48 (–OOCNHCH₂CH₂CH₂CH₂CH₂NHCOO–), 2.44–2.63 (–O(CH₂)CHCH₂CO–), 3.13 (–OOCNHCH₂CH₂CH₂CH₂CH₂NHCOO–), 3.41 (–O(CH₂)CHCH₂O–), 3.46 (–O(CH₂)CHCH₂O–), 3.64 (–OCH₂CH₂O–), 4.20 (–OOCNHCH₂CH₂CH₂CH₂CH₂NHCOO–), 5.21–5.29 (–O(CH₂)CHCH₂CO–). ¹³C NMR of EPH2 (CDCl₃) of poly(PEG/PPG/PHB urethane)s: δ (ppm) 17.77 (–O(CH₂)CHCH₂O–), 20.14 (–O(CH₂)CHCH₂CO–), 26.69 (–OOCNHCH₂CH₂CH₂CH₂CH₂NHCOO–), 30.26 (–OOCNHCH₂CH₂CH₂CH₂CH₂CH₂NHCOO–),

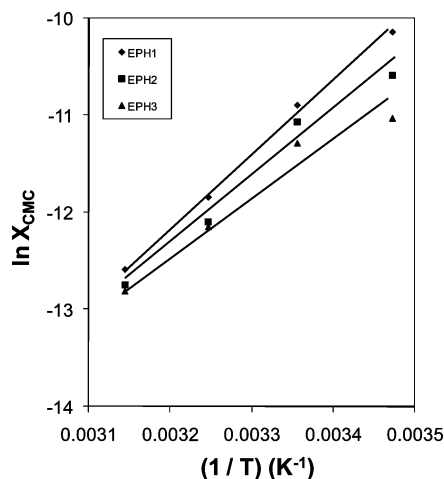
TABLE 2: Thermodynamic Parameters of the Micellization Process of Poly(PEG/PPG/PHB urethane)s

copolymer	temperature (°C)	CMC $\times 10^4$ (g/mL)	ΔG (kJ/mol)	ΔS (kJ/mol/K)	ΔH (kJ/mol)
EPH1	15	19.95	–23.03	0.300	63.0
	25	9.40	–24.73	0.295	
	35	3.65	–26.88	0.293	
	45	1.73	–28.88	0.289	
EPH2	15	11.54	–24.02	0.282	57.2
	25	7.13	–25.12	0.277	
	35	2.55	–27.45	0.275	
	45	1.32	–28.93	0.271	
EPH3	15	6.89	–25.04	0.252	47.1
	25	5.33	–25.62	0.246	
	35	2.25	–27.58	0.244	
	45	1.16	–29.09	0.241	

NHCOO–), 41.20 (–O(CH₂)CHCH₂CO–), 64.18 (–OOCNHCH₂CH₂CH₂CH₂CH₂NHCOO–), 67.99 (–O(CH₂)CHCH₂CO–), 70.94 (–OCH₂CH₂O–), 73.56 (–O(CH₂)CHCH₂O–), 75.72 (–O(CH₂)CHCH₂O–), 156.82 (–OOCNHCH₂CH₂CH₂CH₂CH₂NHCOO–), 169.98 (–O(CH₂)CHCH₂CO–).

Molecular Characterization. Gel permeation chromatography (GPC) analysis was carried out with a Shimadzu SCL-10A and LC-8A system equipped with two Phenogel 5 μ m 50 and 1000 Å columns (size: 300 \times 4.6 mm) in series and a Shimadzu RID-10A refractive index detector. THF was used as eluent at a flow rate of 0.30 mL/min at 40 °C. Monodispersed poly(ethylene glycol) standards were used to obtain a calibration curve. The ¹H NMR (400 MHz) and ¹³C NMR (100 MHz) spectra were recorded on a Bruker AV-400 NMR spectrometer at room temperature. The ¹H NMR measurements were carried out with an acquisition time of 3.2 s, a pulse repetition time of 2.0 s, a 30° pulse width, a 5208 Hz spectral width, and 32K data points. Chemical shift was referred to the solvent peak (δ = 7.3 ppm for CHCl₃). Sodium 3-trimethylsilylpropanesulfonate was used as the internal standard for the measurements conducted in D₂O.

CMC Determination. The CMC values were determined by using the dye solubilization method at 15, 25, 35, and 45 °C.²² The hydrophobic dye 1,6-diphenyl-1,3,5-hexatriene (DPH) was dissolved in methanol with a concentration of 0.6 mM. A 20 μ L portion of this solution was mixed with 2.0 mL of copolymer aqueous solution with concentrations ranging from 0.0001 to 0.5 wt % and equilibrated overnight at 4 °C. A UV–vis spectrophotometer was used to obtain the UV–vis spectra in the range of 330–430 nm at 15, 25, 35, and 45 °C. The CMC

**Figure 1.** Plot of $\ln X_{\text{CMC}}$ against $(1/T)$ for the determination of $\Delta H_{\text{micellization}}$ of the EPH series of copolymers.

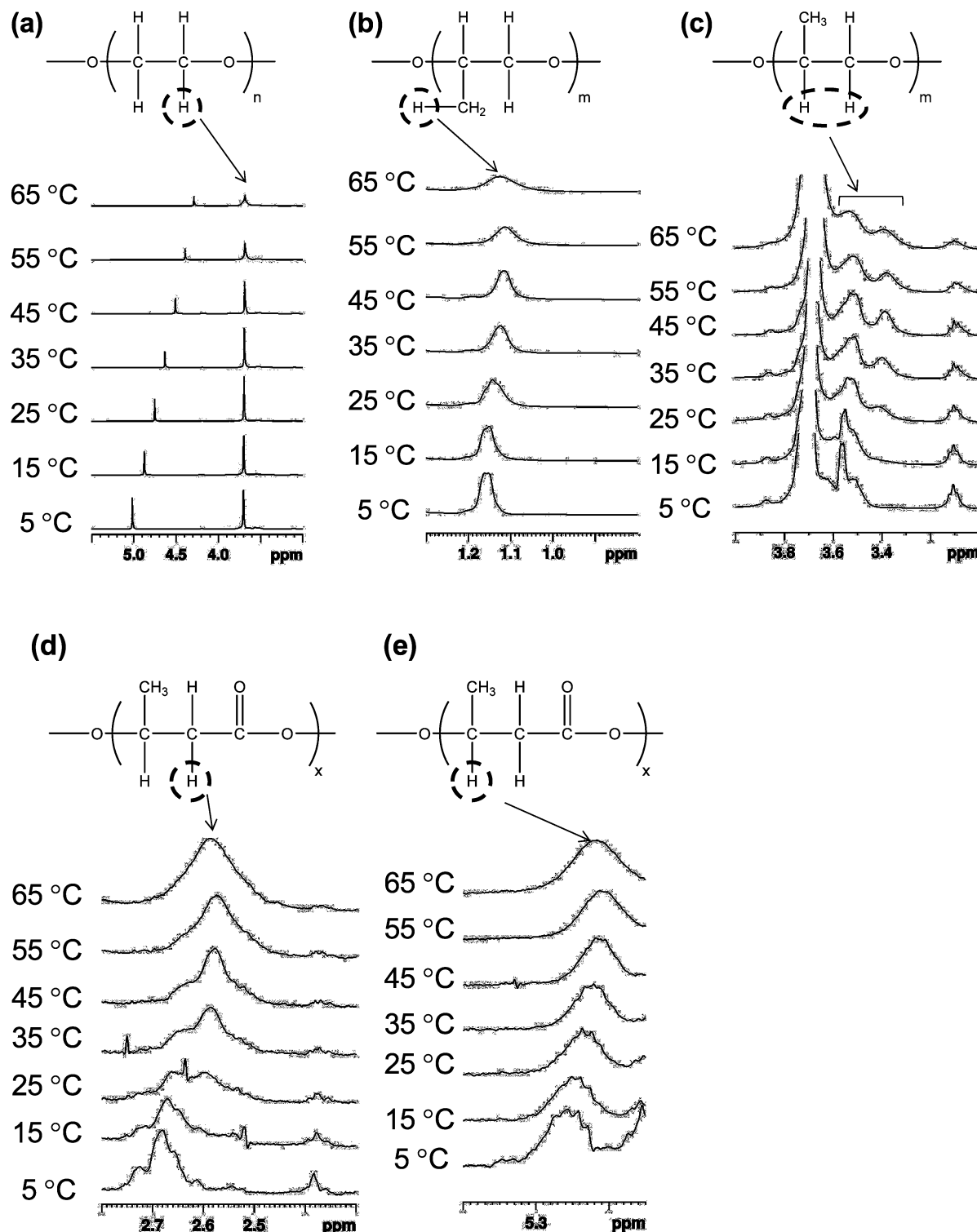


Figure 2. ^1H NMR spectrum of specific segments of (a) PEG, (b, c) PPG, and (d, e) PHB of the poly(PEG/PPG/PHB urethane) copolymer EPH1 at 5 wt % in D_2O at different temperatures.

value was determined by the plot of the difference in absorbance at 378 and 400 nm ($A_{378} - A_{400}$) versus logarithmic concentration.

Atomic Force Microscopy. A Digital Instruments MultiMode atomic force microscope with a Nanoscope IV controller in tapping mode was employed to image the gel samples. Gel samples were prepared from 5 wt % copolymer solution and were incubated at 37 °C for 3 h prior to the experiment. Briefly, silicon disks were soaked in 50% acetone for a minimum of 2 h and rinsed with distilled water. When the silicon disk was completely dried, a thin layer of the gel was coated onto the

disks. The gel was further flattened by pressing a glass coverslip over the silicon disk, and the sample was imaged immediately. All of the atomic force microscopy (AFM) images were obtained with a scan rate of 1 Hz over a selected area of $10\ \mu\text{m} \times 10\ \mu\text{m}$. Image analysis was performed using Nanoscope software after removal of the background slope by flattening the images.

Cell Cultivation. L929 mouse fibroblasts were obtained from ATCC and cultivated in DMEM containing 10% fetal bovine serum (FBS) and 1% penicillin/streptomycin. Cells grew as a monolayer and were passaged upon confluence using trypsin

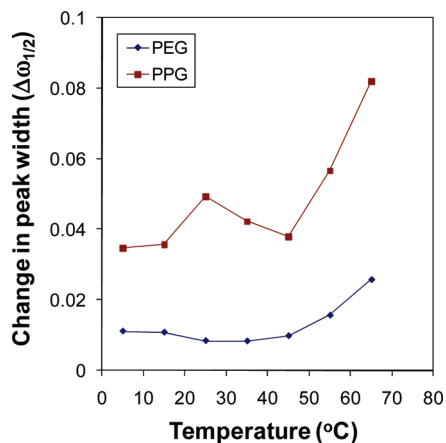


Figure 3. Change in the peak width of the ^1H NMR peaks corresponding to the $-\text{CH}_3$ group of PPG and the $-\text{CH}_2-$ group of PEG in poly(PEG/PPG/PHB urethane) copolymer EPH1 at 5 wt % in D_2O at different temperatures.

(0.5% w/v in PBS). L929 cells were harvested from culture by incubating in trypsin solution for 15 min. The cells were centrifuged, and the supernatant was discarded. A 3 mL portion of serum-supplemented DMEM was added to neutralize any residual trypsin. The cells were resuspended in serum-supplemented DMEM at a concentration of 2×10^4 cells/mL. Cells were cultivated at 37°C and 5% CO_2 .

Cell Growth on Gel Surface. The copolymers (5 wt %) and F127 copolymers (20 wt %) were dissolved in DMEM. At 5 wt %, all of the copolymers formed thermogelling formulations. All copolymer solutions were sterilized by filtration with a $0.45\ \mu\text{m}$ filter before tests. A 0.5 mL portion of the polymer solution was transferred to each well in a 24-well cell culture plate and allowed to incubate at 37°C for 1 h. A 0.5 mL portion of the suspended cell solution was added to each well (10^4 cells/well). The cell culture plate was allowed to incubate for 3 days. Cells were observed using an inverted microscope (Olympus) (magnification = $200\times$) at time intervals of 1, 2, and 3 days.

Cytotoxicity Study of Copolymer. The biocompatibility of the copolymers and F127 copolymers was evaluated by MTT assay in a 96-well cell culture plate. All copolymer solutions were sterilized by filtration with a $0.45\ \mu\text{m}$ filter before tests. The copolymers and F127 copolymers were dissolved in DMEM (maximum concentration: 100 mg/mL). Cells were seeded at a density of 3×10^3 cells/well. Phenol was used as a cytotoxic control. Cells not exposed to any biomaterials were used as a positive control. The plates were incubated at 37°C in a humidified 5% CO_2 atmosphere. After 3 days, 10 mL of 3-(4,5-dimethylthiazol-2-yl)-2,5-diphenyl tetrazolium bromide (MTT) solution (5 mg/mL) was added to each well. After 4 h of incubation at 37°C , the MTT solution was removed and the insoluble formazan crystals that formed were dissolved in 100 mL of dimethylsulfoxide (DMSO). The absorbance of the formazan product was measured at 570 nm using a spectrophotometer (TECAN SpectrofluorPlus).

Extraction of Leachable Products from Gel. A 1 mL portion of polymer gels was placed in a cellulose bag and kept in 50 mL of buffer solution at 37°C in a shaking water bath at 50 rpm. A 2 mL portion of the gel extracts was collected at various time intervals of 1, 3, 7, 14, and 30 days. The solutions were lyophilized, and an equivalent amount of DMEM solution was added to redissolve the residue. All copolymer solutions were sterilized by filtration with a $0.45\ \mu\text{m}$ filter before tests.

Cytotoxicity of Leachable Products from Gel. The biocompatibility of leachable gel products of the copolymers and

F127 copolymers were evaluated by MTT assay. Cells were seeded at a density of 3×10^3 cells/well. A 100 mL portion of the extract solution in DMEM was added to each well. Phenol was used as a cytotoxic control. Cells not exposed to any biomaterials were used as a positive control. The plates were incubated at 37°C in a humidified 5% CO_2 atmosphere. After 3 days, 10 mL of 3-(4,5-dimethylthiazol-2-yl)-2,5-diphenyl tetrazolium bromide (MTT) solution was added to each well. After 4 h of incubation at 37°C , the solutions in the wells were removed and the insoluble formazan crystals that formed were dissolved in 100 mL of dimethylsulfoxide (DMSO). The absorbance of the formazan product was measured at 570 nm using a spectrophotometer (TECAN SpectrofluorPlus).

Results and Discussion

Micelle Formation Properties. The micelle formation properties of the poly(PEG/PPG/PHB urethane)s were studied. The CMC determination was carried out for these copolymers at 15, 25, 35, and 45°C . This experiment was conducted by varying the aqueous polymer concentration in the range 0.0001–0.5 wt %, while keeping the concentration of DPH constant. DPH shows a higher absorption coefficient in a hydrophobic environment than in water. Thus, with increasing polymer concentration, the absorbances at 344, 358, and 378 nm increased. The point where the absorbance suddenly increases corresponds to the concentration at which micelles are formed. When the micelle is formed, DPH partitions preferentially into the hydrophobic core formed in the aqueous solution.^{13,14,16} The CMC was determined by extrapolating the absorbance at 378 nm minus the absorbance at 400 nm ($A_{378} - A_{400}$) versus the logarithmic concentration. The CMC values for the water-soluble copolymers at the different temperatures are tabulated in Table 2.

Assuming a closed association of unimers into micelles, thermodynamic functions such as the molar standard enthalpy, ΔH° , and the entropy, ΔS° , and free energy, ΔG° , for micelle formation can be extracted from the studies of the CMC dependence on temperature.²² The free energy of micellization, ΔG° , can be calculated by

$$\Delta G^\circ = RT \ln(X_{\text{CMC}}) \quad (1)$$

where R is the gas law constant, T is the temperature in K, and X_{CMC} is the CMC in mole fractions at temperature T . The values of ΔG° are negative, indicating the spontaneity of the micellization process. These values are temperature-dependent, becoming more negative at higher temperatures. Further, the values of the standard enthalpy of micellization, ΔH° , and the standard entropy of micellization, ΔS° , can be extracted from the Arrhenius plot of $\ln(X_{\text{CMC}})$ versus $1/T$.

$$\Delta H^\circ = R(d \ln X_{\text{CMC}}/dT^{-1}) \quad (2)$$

$$\Delta S^\circ = (\Delta H^\circ - \Delta G^\circ)/T \quad (3)$$

Figure 1 shows the plot of $\ln X_{\text{CMC}}$ versus T^{-1} . ΔH° was derived from the slope of the linear plot. In all of the solutions studied, enthalpy of micellization was shown to be an endothermic process, similar to aqueous solutions of PEG-PPG-PEG triblock copolymers.²⁸ The enthalpy values became less positive with increasing PHB content, very similar to the previously reported thermogelling poly(PEG/PPG/PLA urethane)s.²² On the

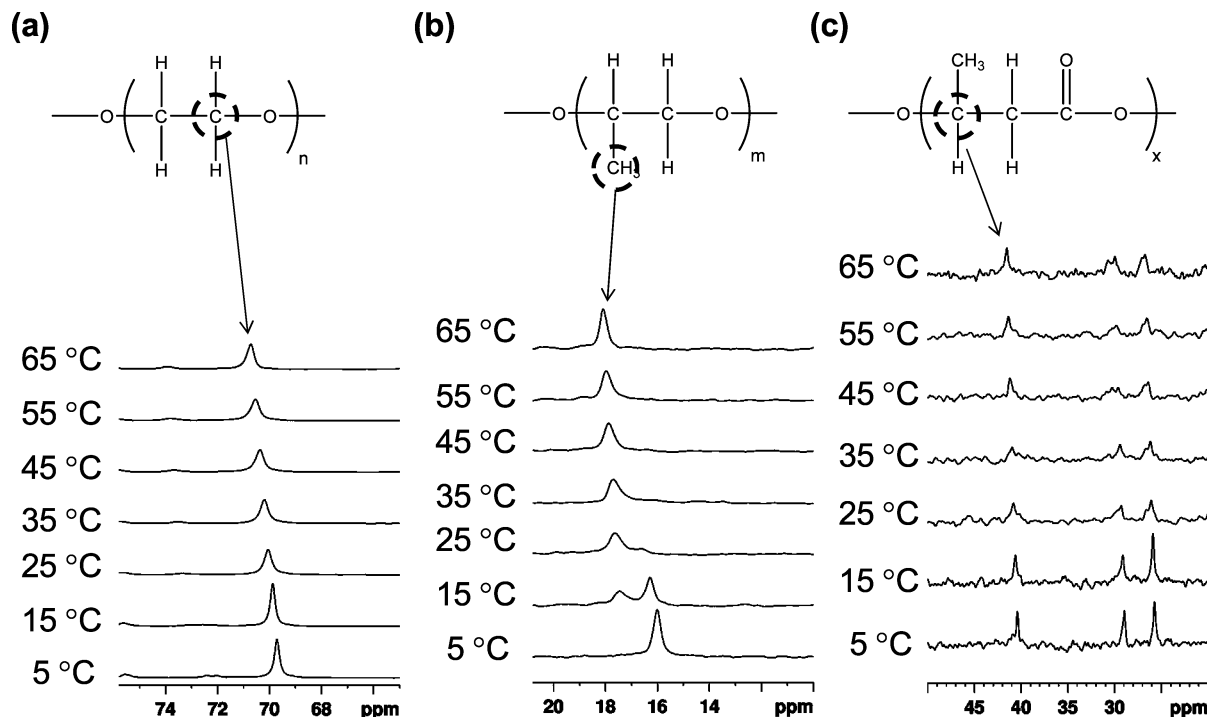


Figure 4. ^{13}C NMR spectrum of specific segments of (a) PEG, (b) PPG, and (c) PHB of poly(PEG/PPG/PHB urethane) copolymer EPH1 at 5 wt % in D_2O at different temperatures.

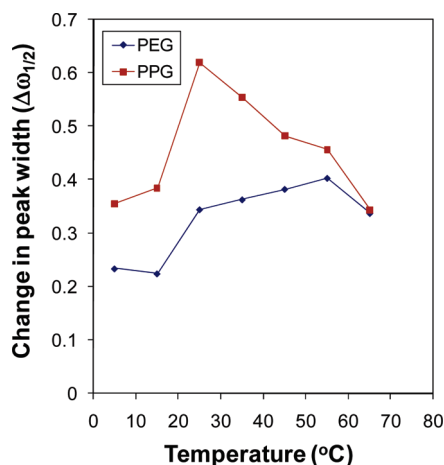


Figure 5. Change in the peak width of the ^{13}C NMR peaks corresponding to the $-\text{CH}_3$ group of PPG and the $-\text{CH}_2-$ group of PEG in poly(PEG/PPG/PHB urethane) copolymer EPH1 at 5 wt % in D_2O at different temperatures.

other hand, the micellization process is entropy-driven, with the value becoming less positive with increasing PHB content. Thus, when the micelles form, ordered water molecules are expelled from the polymer chains, leading to an increase in the entropy.¹⁵ When the PHB content is higher, the association of the polymer chains is greater due to the highly hydrophobic nature of the PHB segments and therefore there is a higher enthalpy gain. However, this leads to a lower extent of interaction with the water molecules and a corresponding decrease in the entropy when the copolymer chains self-assemble into micelles.

Variable Temperature ^1H NMR Studies. The poly(PEG/PPG/PHB urethane)s are water-soluble, and the aqueous copolymer solutions showed thermogelling properties. At low temperatures of around 5–15 °C, the solution has low viscosity and appears clear. Gelation of the solution occurs at about 20 °C, and a clear gel is obtained up to about 50 °C. Above 50 °C, the gel structure collapses and a turbid solution is obtained.

The ^1H NMR spectra of the copolymer solution (EPH1) at 5 wt % in D_2O were recorded at different temperatures. The peak widths corresponding to a specific functional of the copolymers were measured. For PPG, the peak width measurements were done on the peak corresponding to the methyl group of the polymer segment. For PEG, the peak width measurements were done on the peak corresponding to the methylene groups of the polymer segment. Due to the low PHB content and subsequently low signal-to-noise ratio of the peaks, we could not obtain reliable information regarding the change in the peak width of the functional groups of the PHB segments. However, the peak shape changes of the PEG, PPG, and PHB segments are presented in Figure 2. The solution changes from a liquid state to a gel state to a turbid solution as the temperature was raised from 5 to 65 °C. For the PEG protons, there is minimal shift in the peak position from 5 to 45 °C (Figure 2a). Ma et al. have presented a detailed ^1H NMR spectroscopy study on the PEG-PPG-PEG triblock copolymers in D_2O .³⁰ Their work focused on the micellization process of the triblock copolymers with a small section on the gelation of the polymers. Our observation is similar to Ma's observation of the PEG segments for a PEG-PPG-PEG triblock copolymer at high concentrations in D_2O . The peak width at half-height remained fairly constant until above 45 °C, where phase transition occurs. The phase transition led to an increase in the peak width at half-height for the PEG protons. As for the PPG segment, at low temperatures, two doublets corresponding to the methyl and methylene groups of the PPG segment are observed (Figure 2b and c). As the temperature is increased, the peaks broaden. Specifically, for the PPG methyl peak, there is an upfield shift in the methyl peak signal which signals increasing hydrophobicity at higher temperatures.³⁰ There is a sudden increase in the peak width at half-height between 15 and 25 °C upon gelation. This is similar to the observation made by Nivaggioli et al.²⁹ Above 45 °C, phase separation occurs and the peak width at half-height increases again. The change in the peak width of both peaks of PEG and PPG segments in ^1H NMR is reflected in Figure 3.

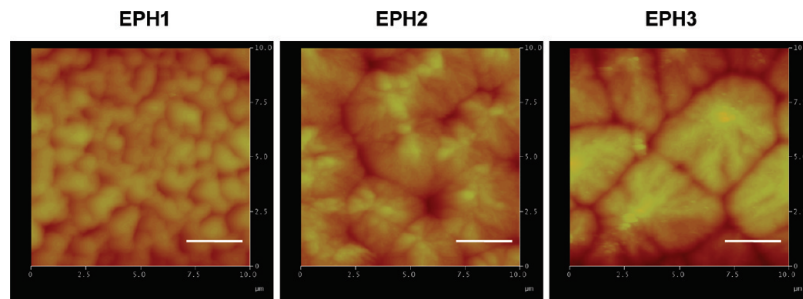


Figure 6. Atomic force microscopy images of the surface of the poly(PEG/PPG/PHB urethane) copolymer gels (scale bar corresponds to 2.5 μm).

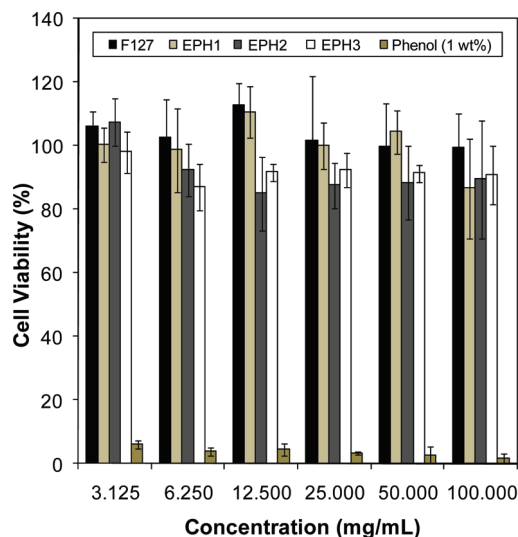


Figure 7. Cell viability plot of various concentrations of poly(PEG/PPG/PHB urethane)s incubated with mouse fibroblast L929 cells for 3 days.

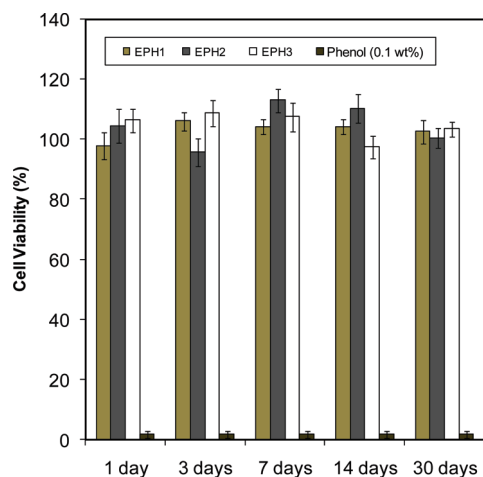


Figure 8. Cell viability plot of the leachable products of poly(PEG/PPG/PHB urethane)s gels obtained after different days.

For the PHB segments, the peak corresponding to the $-\text{CH}_2-$ group appears very different from the typical “doublet of doublet” peaks observed with the spectra in CDCl_3 . This peak shifted upfield and broadened as the temperature was raised. As for the $-\text{CH}-$ group, at low temperatures, a multiplet was discernible. As the temperature was increased, the peaks broadened and the fine features of the peak disappeared.

Variable Temperature ^{13}C NMR Studies. The evidence shown by the ^{13}C NMR spectrum is slightly different from the ^1H NMR spectrum. The changes in the ^{13}C NMR spectrum of EPH1 in D_2O at different temperatures are shown in Figure 4.

A downfield shift was observed for both the methylene groups of PEG and the methyl group of PPG. For the change in the shape of the PPG peak, our observations were similar to that made by Yu et al.³¹ The changes in the peak width of the PEG and PPG segments are shown in Figure 5. Both the PEG and PPG polymer segments display almost the same trend. The peak width increases from 15 to 25 $^\circ\text{C}$, indicating reduced polymer segment motion in the solution. This corresponds to the temperature at which gelation of the copolymer solution occurs. This is similar to the observations made by Yu et al.³¹ The peak width of the polymer segments decreases only between 55 and 65 $^\circ\text{C}$ when the phase separation of the copolymer occurs. It is also interesting to note that the phase separation leads to a broadening of the peaks in the ^1H NMR spectrum and a narrowing of peaks in the ^{13}C NMR spectrum.

Understanding the NMR Results. From both the ^1H and ^{13}C NMR spectrum, the gelation of the copolymer solution leads to a broadening of the peaks. This clearly shows that the movement of the polymer segments is retarded by the gelation process. This is consistent with the observation that the diffusive motion is slowed down in the gel regime of aqueous PEG-PPG-PEG copolymer solutions.³² However, the difference between this copolymer gel and the conventional Pluronic gel is that the former phase separates at a lower temperature. This allows the study of the change in the molecular motion occurring at the phase transition. During the phase separation stage (clear gel to turbid sol stage), a major difference between the ^1H and ^{13}C NMR spectra is observed. The ^1H NMR spectra of both the PEG and PPG segments show a peak broadening, indicating reduced molecular motion. The ^{13}C NMR of both the PEG and PPG segments shows peak narrowing, indicating increased motion. Before phase separation, there is a greater proportion of polymer–water interactions than polymer–polymer interactions. After phase separation, there is a greater proportion of polymer–polymer interactions than polymer–water interactions. The ^1H NMR profile is greatly influenced by the extent of the polymer–water interactions. The interaction between the water molecules and the polymer segments, such as the PEG segment, takes place via the hydrogen bonding interaction between the proton of the polymer segment and the water molecule.^{29,33} Upon the dehydration of the PEG and PPG segments, the polymer–water interactions are reduced, leading to reduced molecular motion of the protons on the copolymer segments. On the other hand, the ^{13}C NMR profile is influenced more significantly by the extent of the polymer–polymer interactions than polymer–water interactions. The carbon atoms of the polymer segment do not interact or are indirectly affected by the surrounding water molecules. Therefore, the molecular motion of these atoms would be less sensitive to changes in the external water environment. Instead, it will be more affected by the phase separation process, leading to increased polymer–polymer

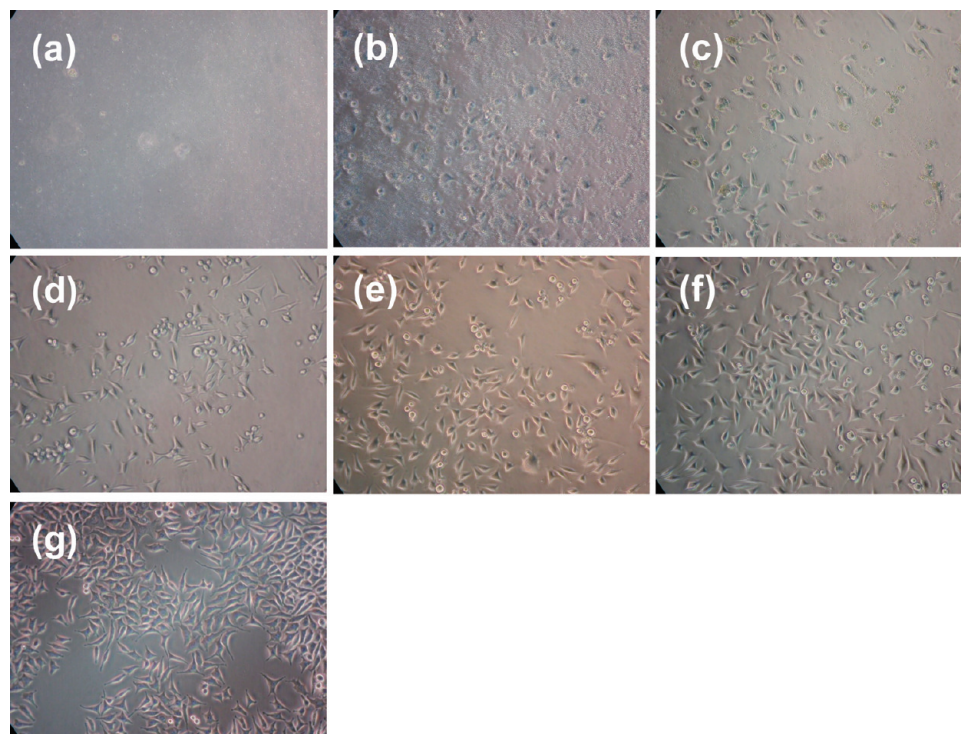


Figure 9. Phase contrast micrographs of L929 cells cultured on Pluronic F127 at different concentrations: (a) 20 wt % (gel state); (b) 15 wt %; (c) 10 wt %; (d) 5 wt %; (e) 2.5 wt %; (f) 1.25 wt %; (g) polystyrene tissue culture dish.

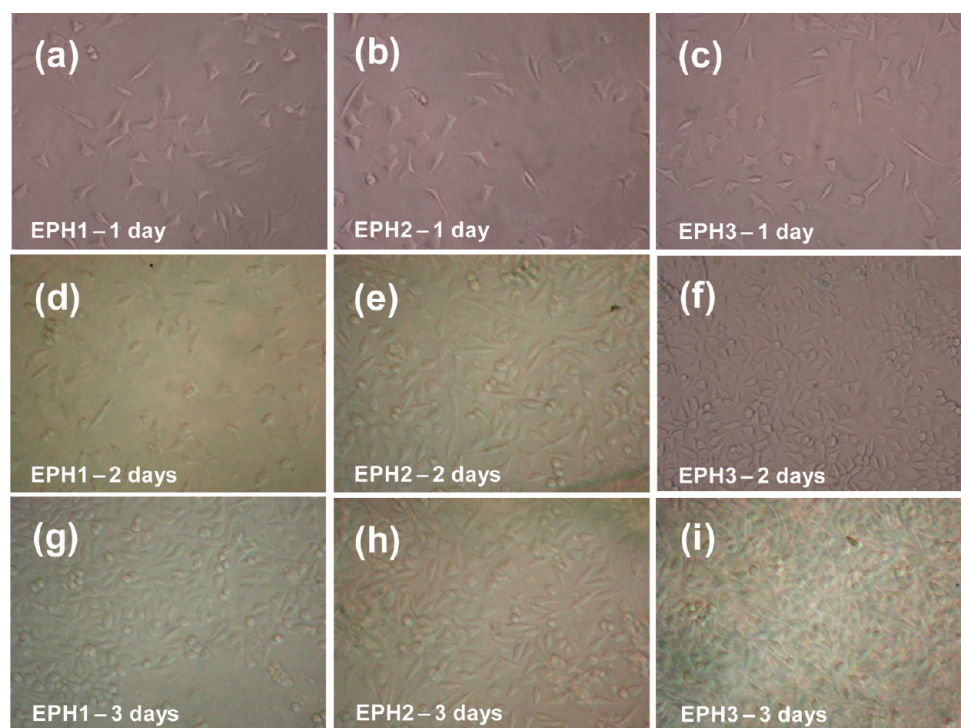


Figure 10. Phase contrast micrographs of L929 cells cultured on poly(PEG/PPG/PHB urethane) gel surface at different periods of incubation.

interactions. When phase separation occurs, the collapse of the polymer chains leads to possible phase blending between the polymer segments. PEG and PPG are known to be compatible polymers.^{34,35} Furthermore, at higher temperatures, the vibrational, rotational, and translational motion of the polymer segments increases; the ^{13}C NMR spectra thus show a narrowing of the peak width. The self-diffusion of the PEG-PPG-PEG triblock copolymer has been reported to show greater self-diffusion coefficients at temperatures higher than 50 °C.³⁴ When the copolymer chains are dehydrated, the copolymer molecules

become more flexible as the solution becomes a mixture resembling a polymer melt containing water.³⁴

AFM Studies. The surfaces of the thermogelling copolymers were observed using AFM. The images are shown in Figure 6. The images show that the gels were assembled from micrometer-sized entities. It is very likely that these entities are made of micelle clusters. The gelation process of Pluronic F127 in water had been suggested to take place via close packing of micellar spheres.³¹ Here, the formation of micelle clusters is likely to be from the self-assembly of micelle spheres. When there is a

sufficiently high concentration of the micelle clusters assembling together, a supramolecular water retaining gel structure is formed. From the micrographs, it can be seen that, as the PHB content increases, the micelle clusters become larger in size. Wanka et al. have previously reported that, for a PEG-PPG-PEG copolymer with the same PPG block length but decreasing PEG block length, the cubic phase, followed by the hexagonal phase, disappears.³³ In the AFM micrographs of the gels, EPH1 shows a nearly worm-like structure made of spherical particles. The surface structure of this gel appears to be on the boundary of the cubic and the hexagonal phase. EPH2 shows a better defined worm-like structure. Interestingly, an AFM image of the Pluronic F127 copolymer (1 wt %) coated on untreated silicon substrate shows a very similar morphology to the AFM image of EPH2 gel.³⁶ EPH3 shows a nearly lamellar structure. From our critical gelation concentration studies reported previously, we found that the critical gelation concentration is the highest for EPH3, followed by EPH1, followed by EPH2. From here, it appears that the worm-like hexagonal packing gives the most efficient packing for the gels, leading to the lowest critical gelation concentration.

In Vitro Cytotoxicity. The cytotoxicity of the polymers was tested at various concentrations ranging from 3.125 to 100 mg/mL using the mouse fibroblast L929 cells. Quantification of the cytotoxic response was done using the MTT assay (Figure 7). In general, the polymers do not show significant toxicity. It is important to note that, at concentrations above 12.5 mg/mL, the solution becomes viscous or even in a gel state. It means that, even when the cells are in the interior of the gel, they remain viable. These results show that, potentially, these cells can be encapsulated for 3D-cell growth.

The cytotoxicity of the leachable products from the copolymer gel was evaluated by incubating the gel in the cell culture medium over a period of 30 days at 37 °C. The aim of this experiment is to simulate the actual usage conditions when the gel is injected. Quantification of the cytotoxic response was done using the MTT assay (Figure 8). Aqueous extracts of the copolymer gel do not show significant cytotoxicity against L929 cells, regardless of the incubation length. The use of dibutyltin dilaurate as a catalyst raises a safety concern, particularly when it is a known cytotoxic chemical. In our cytotoxicity test of this chemical, we observed that below a concentration of 1 ppm, this chemical does not elicit a cytotoxic response against the L929 mouse fibroblast cells. In this work, we determined the tin content in the copolymer to be below 1 ppm by UV absorption studies of the copolymer dissolved in chloroform as well as NMR. From the MTT assay results of the leachable extracts of the copolymer gels and the determined tin content in the copolymer, the gels are expected to be safe for biomedical applications.

Cell Growth on Gel Surface. The cell growth on the gel surfaces was tested. On the Pluronic F127 (20 wt %) gel surface, the cells did not attach well to the surface. The almost smooth morphology observed in the micrograph was due to the difficulty in capturing the image of the floating cells (Figure 9a). This is similar to the observation made previously.²⁴ That study showed faint images of the cells. At a concentration of 15 wt %, the solution was viscous but not in a gel state (Figure 9b). In this state, some of the cells were observed to be attached and some were observed to be rounded. At even lower concentrations, the extent of attachment of the cells increased (Figure 9c–g). The number of attached cells was observed to be higher as the concentration of Pluronic F127 became lower. These results indicate the excellent biocompatibility of Pluronic F127.

Fibroblast cell growth on the surface of the poly(PEG/PPG/PHB urethane) gels appears to be more promising (Figure 10). After 24 h of incubation, we observed the typical spindle-like fibroblast morphology (Figure 10a–c). The cells were incubated for up to 72 h. For the copolymer gels, the cell numbers were found to increase up to 72 h (Figure 10g–i). Moreover, the cells maintained a healthy morphology. However, for the Pluronic F127 gel, the cell growth was suppressed at longer time periods. It has been previously reported that the cell growth on hydrophilic surfaces is not favorable and such a surface would inhibit the growth of cells.³⁷ On the other hand, PHB has been reported to be compatible to cells such as osteoblastic cells, epithelial cells, and ovine chondrocytes.^{38,39} Recently, we showed excellent fibroblastic proliferation in the presence of PNIPAAm-PHB-PNIPAAm block copolymers in solution.⁴⁰ In addition, these triblock copolymers were compatible with human mesenchymal stem cells and mouse embryonic stem cells.^{41,42} Poly(PEG/PPG/PCL urethane)s also appear to be nontoxic to cells.⁴³ Therefore, the incorporation of the PHB segment to the PEG and PPG segments greatly enhances the cell adhesion capability of the copolymer gel. The incorporation of PHB into the copolymers could have increased the hydrophobicity of the copolymer gel surface compared with Pluronic F127 gel. Both Pluronic F127 and the poly(PEG/PPG/PHB urethane) copolymers are nontoxic to cells. However, this is not sufficient for good cell adhesion. This study shows that the surface properties of the gels are crucial requirements for the favorable adhesion of cells onto the gels. This is an important finding which has possible implications in the design of materials for tissue engineering and the engineering of biomaterials for *in vivo* applications.

Conclusions

The thermodynamics of micellization of multiblock poly(ester urethane)s having poly[(*R*)-3-hydroxybutyrate] (PHB), poly(ethylene glycol) (PEG), and poly(propylene glycol) (PPG) segments was studied. Micelle formation was found to be entropy-driven. The gelation of the thermogelling copolymers was studied by variable temperature ¹H and ¹³C NMR spectroscopy. Macroscopic observations of the gelation process were related to the NMR results. Using AFM, we observed micrometer-sized entities which could possibly be micelle clusters. Further, it appears that the formation of the gel is due to the aggregation of micelle clusters. A higher content of PHB increased the size of the micelle cluster. Cytotoxicity studies performed on the copolymer or the extracts of the copolymer gel indicate good cell compatibility. Excellent cell attachment was observed on the surface of the gel. The results are significantly better than those on the commercially available PEG-PPG-PEG triblock copolymer. These studies indicate a potential for the copolymer gel to be used for tissue engineering applications or for 3D cell culture.

Acknowledgment. The authors acknowledge the financial support from Institute of Materials Research and Engineering, A*STAR, Singapore (IMRE/06-1R0529), and National University of Singapore (R-397-000-019-112). The authors thank M. J. Loh and J. G. Lim for kindly proofreading the manuscript. X.J.L. would like to acknowledge the A*STAR Graduate Scholarship from A*STAR.

References and Notes

- (1) Huang, K.; Lee, B. P.; Ingram, D. R.; Messersmith, P. B. *Biomacromolecules* **2002**, *3*, 397–406.

- (2) Daga, A.; Muraglia, A.; Quarto, R.; Cancedda, R.; Corte, G. *Gene Ther.* **2002**, *9*, 915–921.
- (3) Packhaeuser, C. B.; Schnieders, J.; Oster, C. G.; Kissel, T. *Eur. J. Pharm. Biopharm.* **2004**, *58*, 445–455.
- (4) Heller, J.; Barr, J.; Ng, S. Y.; Shen, H. R.; Abdellaoui, S.; Gurny, R.; Castioni, N. V.; Loh, P. J.; Baehni, P.; Mombelli, A. *Biomaterials* **1999**, *23*, 4397–4404.
- (5) Hill-West, J. L.; Chowdhury, S. M.; Slepian, M. J.; Hubbell, J. A. *Proc. Natl. Acad. Sci. U.S.A.* **1994**, *91*, 5967–5971.
- (6) Yokoyama, M. *Crit. Rev. Ther. Drug Carrier Syst.* **1992**, *9*, 213–248.
- (7) Loh, X. J.; Li, J. *Expert Opin. Ther. Pat.* **2007**, *17*, 965–977.
- (8) Gilbert, J. C.; Hadgraft, J.; Bye, A.; Brookes, L. *Int. J. Pharm.* **1986**, *32*, 223–228.
- (9) Nalbandian, R. M.; Henry, R. L.; Wilks, H. S. *J. Biomed. Mater. Res.* **1972**, *6*, 583–590.
- (10) Exner, A. A.; Krupka, T. Y.; Scherrer, K.; Teets, J. M. *J. Controlled Release* **2005**, *106*, 188–197.
- (11) Esposito, E.; Carotta, Y.; Scabbia, A.; Trombelli, L.; D'Antona, P.; Menegatti, E.; Nastruzzi, C. *Int. J. Pharm.* **1996**, *142*, 9–23.
- (12) Katakam, M.; Ravis, W. R.; Golden, D. L.; Banga, A. K. *Int. J. Pharm.* **1997**, *152*, 53–58.
- (13) Bae, S. J.; Suh, J. M.; Sohn, Y. S.; Bae, Y. H.; Kim, S. W.; Jeong, B. *Macromolecules* **2005**, *38*, 5260–5265.
- (14) Hwang, M. J.; Suh, J. M.; Bae, Y. H.; Kim, S. W.; Jeong, B. *Biomacromolecules* **2005**, *6*, 885–890.
- (15) Jeong, B.; Bae, Y. H.; Kim, S. W. *Colloids Surf., B* **1999**, *16*, 185–193.
- (16) Jeong, B.; Bae, Y. H.; Kim, S. W. Thermoreversible gelation of PEG-PLGA-PEG triblock copolymer aqueous solutions. *Macromolecules* **1999**, *32*, 7064–7069.
- (17) Jeong, B.; Bae, Y. H.; Lee, D. S.; Kim, S. W. Biodegradable block copolymers as injectable drug-delivery systems. *Nature* **1997**, *388*, 860–862.
- (18) Jeong, B.; Kibbey, M. R.; Birnbaum, J. C.; Won, Y. Y.; Gutowska, A. Thermogelling biodegradable polymers with hydrophilic backbones: PEG-g-PLGA. *Macromolecules* **2000**, *33*, 8317–8322.
- (19) Joo, M. K.; Sohn, Y. S.; Jeong, B. Stereoisomeric effect on reverse thermal gelation of poly(ethylene glycol)/poly(lactide) multiblock copolymer. *Macromolecules* **2007**, *40*, 5111–5115.
- (20) Loh, X. J.; Goh, S. H.; Li, J. *Biomacromolecules* **2007**, *8*, 585–593.
- (21) Loh, X. J.; Goh, S. H.; Li, J. *Biomaterials* **2007**, *28*, 4113–4123.
- (22) Loh, X. J.; Tan, Y. X.; Li, Z.; Teo, L. S.; Goh, S. H.; Li, J. *Biomaterials* **2008**, *29*, 2164–2172.
- (23) He, C.; Kim, S. W.; Lee, D. S. *J. Controlled Release* **2008**, *127*, 189–207.
- (24) Higuchi, A.; Yamamoto, T.; Sugiyama, K.; Hayashi, S.; Tak, T. M.; Nakagawa, T. *Biomacromolecules* **2005**, *6*, 691–696.
- (25) Li, X.; Loh, X. J.; Wang, K.; He, C.; Li, J. *Biomacromolecules* **2005**, *6*, 2740–2747.
- (26) Loh, X. J.; Tan, K. K.; Li, X.; Li, J. *Biomaterials* **2006**, *27*, 1841–1850.
- (27) Loh, X. J.; Wang, X.; Li, H.; Li, X.; Li, J. *Mater. Sci. Eng., C* **2007**, *27*, 267–273.
- (28) Alexandridis, P.; Holzwarth, J. F.; Hatton, T. A. *Macromolecules* **1994**, *27*, 2414–2425.
- (29) Nivaggioli, T.; Tsao, B.; Alexandridis, P.; Hatton, T. A. *Langmuir* **1995**, *11*, 119–126.
- (30) Ma, J.; Guo, C.; Tang, Y.; Liu, H. *Langmuir* **2007**, *23*, 9596–9605.
- (31) Yu, G.-E.; Deng, Y.; Dalton, S.; Wang, Q.-G.; Attwood, D.; Price, C.; Booth, C. *J. Chem. Soc., Faraday Trans.* **1992**, *88*, 2537–2544.
- (32) Walderhaug, H.; Nystrom, B. *J. Phys. Chem. B* **1997**, *101*, 1524–1528.
- (33) Wanka, G.; Hoffmann, H.; Ulbricht, W. *Macromolecules* **1994**, *27*, 4145–4159.
- (34) Fleischer, G.; Bloss, P.; Hergeth, W. D. *Colloid Polym. Sci.* **1993**, *271*, 217–222.
- (35) Morales, E.; Salmeron, M.; Acosta, J. L. *J. Polym. Sci., Part B: Polym. Phys.* **1996**, *34*, 2715–2721.
- (36) Wu, C. H.; Liu, T. B.; White, H.; Chu, B. *Langmuir* **2000**, *16*, 656–661.
- (37) Higuchi, A.; Tamiya, S.; Tsubomura, T.; Katoh, A.; Cho, C. S.; Akaike, T.; Hara, M. *J. Biomater. Sci., Polym. Ed.* **2000**, *11*, 149–168.
- (38) Nebe, B.; Forster, C.; Pommerenke, H.; Fulda, G.; Behrend, D.; Bernewski, U.; Schmitz, K. P.; Rychly, J. *Biomaterials* **2001**, *22*, 2425–2434.
- (39) Rivard, C. H.; Chaput, C.; Rhalmi, S.; Selmani, A. *Ann. Chir.* **1996**, *50*, 651–658.
- (40) Loh, X. J.; Zhang, Z. X.; Wu, Y. L.; Lee, T. S.; Li, J. *Macromolecules* **2009**, *42*, 194–202.
- (41) Loh, X. J.; Cheong, W. C. D.; Li, J.; Ito, Y. *Soft Matter* **2009**, *5*, 2937–2946.
- (42) Loh, X. J.; Gong, J.; Sakuragi, M.; Kitajima, T.; Liu, M.; Li, J.; Ito, Y. *Macromol. Biosci.* [Online early access]. DOI: 10.1002/ma-bi.200900081. Published Online June 15, **2009**.
- (43) Loh, X. J.; Sng, K. B. C.; Li, J. *Biomaterials* **2008**, *29* (22), 3185–3194.

JP903984R